NASA TECHNICAL MEMORANDUM

NASA TM X-2841

NASA TM X-2841

FULL-SCALE EXPERIMENTS WITH AN EJECTOR TO REDUCE JET ENGINE EXHAUST NOISE

by Bruce J. Clark

Lewis Research Center

Cleveland, Ohio 44135

NATIONAL AERONAUTICS AND SPACE ADMINISTRATION • WASHINGTON, D. C. • AUGUST 1973

1. Report No.	2. Government Accession No.	3. Recipient's Catalog No.
NASA TM X-2841		

4. Title and Subtitle	5. Report Date
FULL-SCALE EXPERIMENTS WITH AN EJECTOR TO REDUCE JET ENGINE EXHAUST NOISE	August 1973
	6. Performing Organization Code

7. Author(s)	8. Performing Organization Report No.
Bruce J. Clark	E-7445
	10. Work Unit No. 765-69

9. Performing Organization Name and Address	11. Contract or Grant No.
Lewis Research Center National Aeronautics and Space Administration Cleveland, Ohio 44135	
	13. Type of Report and Period Covered
12. Sponsoring Agency Name and Address	Technical Memorandum
National Aeronautics and Space Administration Washington, D.C. 20546	14. Sponsoring Agency Code

15. Supplementary Notes

16. Abstract

Experiments with a modified J65 turbojet engine and ejector resulted in noise power reductions as large as 13 decibels in the low-frequency range. High-frequency noise power, which appeared to originate mainly from the mixing processes within the ejector, increased. Peak velocities at the ejector exit were reduced by one-half to two-thirds, although survey rakes showed that mixing was not complete. Acoustical lining inside the ejector would reduce the perceived noise level (in PNdB) by removing much of the high-frequency noise.

17. Key Words (Suggested by Author(s))	18. Distribution Statement
Jet engine noise Noise reduction Acoustics	Unclassified - unlimited

19. Security Classif. (of this report)	20. Security Classif. (of this page)	21. No. of Pages	22. Price*
Unclassified	Unclassified	30	$3.00

* For sale by the National Technical Information Service, Springfield, Virginia 22151

FULL-SCALE EXPERIMENTS WITH AN EJECTOR TO REDUCE JET ENGINE EXHAUST NOISE

by Bruce J. Clark

Lewis Research Center

SUMMARY

Tests with a J65 turbojet engine fitted with an annular exhaust nozzle and an ejector 4.88 meters long showed a noise pattern that corresponded to an intense internal mixing region generating high-frequency noise, followed by a less intense and lower frequency noise-producing region at the ejector exit. The low-frequency noise power in the direction of the jet exhaust was as much as 13 decibels below that produced by a standard conical nozzle. The high-frequency noise power increased by about 7 decibels and radiated out both the inlet and the exit of the ejector. Much of this high-frequency noise could be removed by acoustically lining the inner surfaces of the ejector.

Total pressure and temperature profiles show that substantial, but not complete, mixing occurred within the confines of the ejector. With a secondary- to primary-flow-area ratio of 5, the maximum velocity at the exit was reduced by two-thirds. Comparison of measured flow and thrust with calculated values shows a discrepancy that can be partly accounted for by drag and friction losses.

INTRODUCTION

In spite of the trend toward turbofan engines for commercial aviation in the last several years, the exhaust noise of fan and jet aircraft remains a serious problem. Community awareness and more frequent flights are forcing a tighter regulation of allowable aircraft noise. Development of future supersonic aircraft for commercial use will require priority consideration of the jet exhaust noise problem.

A device frequently considered for exhaust noise reduction is an ejector. In the ejector the primary engine exhaust induces and then mixes with a secondary flow of cold ambient air to produce a mixed flow of lower velocity and temperature.

Ejector designs for aircraft exhausts (refs. 1 to 9) usually result in small secondary flows because of the comparatively short length allowed for mixing and the small area available for induced flow. Typically, the induced secondary flows represent a 30 percent increase in the total mass flows. Measured noise power (PWL) reductions are only about 5 decibels. The degree of mixing and the noise reduction can be enhanced by subdividing the primary flow by means of multiple tubes or a "daisy" cross section.

Calculations based on a one-dimensional model of the mixing process indicate that 20 to 25 decibels of noise power reduction should be possible. These calculations assume that an ejector which is long enough for complete mixing to occur has small secondary inlet losses and has a secondary flow area several times larger than the primary flow area. Under some conditions, small-scale cold air jet tests (refs. 10 to 11) with such ejectors show as much as 10 decibels diminution.

To evaluate an ejector at full scale and with hot gas ($\leq 600^{\circ}$ C), the present tests were undertaken with a J65 turbojet engine exhaust and an appropriately sized ejector. Because of the 4.88-meter length required, this ejector is impractical for use on an aircraft. These large-scale tests allow installation of numerous pressure and temperature rakes to obtain a detailed picture of the internal flow fields.

To shorten the ejector length required to obtain complete mixing, the primary flow was introduced through an annulus around a centerbody. The induced secondary flow entered through a bell-mouth and a larger annulus around the primary. The theoretical calculations indicated that considerably more secondary flow (and less noise) would result from employing a diffuser at the end of the mixing section; this was accomplished conveniently by ending the centerbody with a spike.

Sound pressure level (SPL) measurements were made during tests with a standard J65 engine, as well as the J65 plus ejector. Angular and spectral noise level comparisons could then be made at identical engine speed settings.

The thrusts of the engine and ejector were measured separately to determine whether the calculated thrust increment was achieved.

This report summarizes noise and flow measurements made at engine speeds from 50 to 100 percent of maximum (8300 rpm). In this operating range, turbine exhaust temperatures varied from 422° to 678° C, and exhaust pressures from 1.07 to 2.29 atmospheres.

ENGINE AND MEASUREMENT EQUIPMENT

For tests in this study we used a J65 turbojet engine mounted on a thrust stand in an area free of acoustic reflections (figs. 1 and 2). The engine inlet was acoustically treated to minimize radiation of compressor noise. A large ejector was mounted close behind the engine on a separate thrust stand. This ejector was instrumented for pressure

and temperature in order to determine the internal flow fields. Microphones were placed on a 30.5-meter radius in the front quadrant and on a 61-meter radius in the rear quadrant. At each engine speed setting, flow and noise measurements were recorded for later analysis.

J65 Engine Configurations

The J65 engine, its test stand, and the acoustically treated inlet were the same as those used in studies of inlet noise suppression (ref. 12). The centerline height of the engine was 1.07 meters. The inlet with acoustical treatment on four radial struts and the splitter ring as well as on the outer cowling gave the most inlet noise suppression of those tested. Hence, it was chosen for use in the present studies.

For noise comparison purposes, a standard 49.6-centimeter-diameter exhaust nozzle was tested first. For matching to the ejector, the exhaust nozzle was changed to a 8.9-centimeter-wide annulus around a 56.6-centimeter-diameter centerbody, equivalent in area to a 48.2-centimeter-diameter conventional nozzle. The following table shows points taken from the performance map for the J65 engine (ref. 13). Velocities are calculated for each total temperature and pressure. Maximum rated speed for the J65 engine is 8300 rpm.

	Engine speed, percent of maximum			
	80	90	95	100
Standard nozzle (area, 0.192 m^2):				
Exhaust total temperature, ^{o}C	235	396	474	555
Exhaust total pressure, atm	1.190	1.665	1.895	2.11
Calculated exhaust velocity, m/sec	227	436	512	579
Annular nozzle (area, 0.183 m^2):				
Exhaust total temperature, ^{o}C	295	485	571	652
Exhaust total pressure, atm	1.30	1.825	2.075	2.31
Calculated exhaust velocity, m/sec	293	502	578	644

Ejector Details

As shown in figures 2 and 3, the ejector was a 131-centimeter-diameter steel pipe 4.88 meters in length, with a bell-mouth inlet of Fiberglas. The cylindrical portion of the ejector commenced at the engine outlet plane with a 56.6-centimeter-diameter pipe

extending half the length of the ejector and terminating in a spike. This centerbody and spike were supported by 3.8-centimeter-diameter struts. The original fairings around these struts failed in initial tests; and for the results reported herein, all fairings were removed. Geometrical relations in the ejector are summarized in the following table:

	Inner diameter, cm	Outer diameter, cm	Passage height, cm	Area, cm^2
Primary flow passage	56.6	74.3	8.9	1 823
Secondary flow passage	74.6	131	28.1	9 080
Mixed flow passage	56.6	131	37.2	10 920
Ejector exhaust passage	0	131	65.5	13 440

The length along the ejector of 2.44 meters corresponds to 27 passage heights for the primary flow and 8.7 passage heights for the secondary flow. The secondary- to primary-flow-area ratio of the ejector is 5. The mixed flow area includes primary and secondary flow areas, and in addition a small base area resulting from the thickness of the wall separating these flows.

The axial thrust of the ejector was measured separately from the engine thrust. A slight gap in the centerbody (fig. 3) prevented transmission of the ejector thrust to the engine. The vertical support rods for the ejector (fig. 2) were pivoted at top and bottom.

Flow Instrumentation

Total pressure and total temperature probes were installed at the primary and secondary inlets and at successive stations along the ejector length (fig. 3). Probe ends on the rakes were spaced to occur at equal increments of area; most rakes consisted of five individual probes. Total temperatures were measured by Chromel-Alumel thermocouples which were unshielded, except those on the first rake in the hot J65 exhaust. Wall temperatures were also measured by Chromel-Alumel thermocouples. All pressures, including static pressures along the walls, were sensed in sequence by strain-gage-type transducers and recorded remotely on a strip chart. Temperatures were similarly recorded in sequence.

Sound Measurements

Seventeen microphones were distributed at 10° increments in angular position from the engine inlet axis to 20° from the exhaust axis (fig. 1). Those in the front quadrant (0° to 90°) were placed on a 30.5-meter radius; those in the rear quadrant (90° to 160°) were placed on a 61-meter radius, since the sound sources in the exhaust were distributed over such a large distance. The reference point in all cases was at the end of the standard exhaust nozzle on the J65 engine. All microphones were 1.07 meters above the ground. Sound pressure level measurements from the microphones at 61 meters were normalized to the 30.5-meter distance by adding 6 decibels to correct for inverse-square losses.

Commercial 1.27-centimeter condenser microphones were used which, with compensation and matched amplifiers, gave essentially flat responses to 20 kilohertz. Correction for losses at high frequencies in the long microphone cables were made in the data reduction. A pistonphone calibrator generating 124 decibels was used to calibrate each microphone system each day prior to tests.

Reported sound pressure level measurements are the average of five samples taken in two days. All SPL are referenced to 0.0002 microbar, and all PWL to 0.1 picowatt. Sound measurements were not taken when wind speeds exceeded 6 meters per second.

RESULTS AND DISCUSSION

The overall PWL produced with the ejector shroud (with annular nozzle and centerbody) showed a noise reduction of as much as 8 decibels in the rear quadrants (exhaust noise) at the higher engine speeds compared to that produced by the standard J65 exhaust nozzle. Noise in the forward quadrants was increased as much as 10 decibels by adding the ejector. Total noise with the ejector increased over that for the standard nozzle at lower speeds, but at higher speeds it decreased as much as 6 decibels. Spectral noise power data indicated that, with the ejector, low-frequency noise was attenuated and high-frequency noise increased in the exhaust direction. With the ejector, the noise level in the forward direction was raised throughout the spectrum, chiefly in the higher frequencies. These results can be explained in part by a high level of internal noise generated by the mixing of primary and secondary flow within the ejector. Flow measurements indicated that incomplete mixing occurred in these experiments.

Ejector Flow Surveys

The particular geometry of this ejector resulted in a mixing length-width ratio of 27 for the primary flow and 8.7 for the secondary flow, not including the diffuser section. Figure 4 shows pressure, temperature, and velocity profiles at maximum engine speed (100 percent). Surveys at other speeds are similar in shape. It is apparent that inadequate time or length was allowed for the secondary flow to mix out uniformly. It appears from the decrement in core velocity at the 1.2-meter station, and from the region of undisturbed secondary flow, that the mixing zone spread at approximately the 7^{o} half-angle typical of unconfined jets. This is also indicated by the wall temperature profile of figure 5; a sharp increase in heat transfer to the wall occurred at about 2.1 meters.

Although uniform mixing was not achieved, the considerable reduction in velocity from that of the initial primary flow is apparent. Figure 6 shows the variation along the ejector length of the peak values of total pressure and temperature and the corresponding velocity peaks. At the exit the peak velocities are approximately one-third to one-half those of the entering primary stream.

In figure 7 the performance of the J65 engine with the ejector, as a function of engine speed, is compared to that predicted by the one-dimensional calculation procedure shown in the appendix. The discrepancy in flow may be caused by skin friction at the walls and wake losses at supporting struts, as well as by mixing deficiencies. Calculations of secondary flow static pressure, mixed flow total pressure, and total thrust of engine and ejector were made for various drag coefficients C_D associated with the cylindrical support struts in the flow passage. The friction losses on the outer and inner walls of the flow passage are also included for various friction factors. Comparison of the measured values of static pressure in the secondary flow with the calculated static pressures (fig. 7(a)) shows rough agreement with an assumed C_D of 1.0 for the struts and a friction factor f of 0.01. Total pressures across the annulus of mixed flow are averaged and compared with the calculated values at corresponding primary flows (fig. 7(b)). The measured results tend to agree with the calculated curve for $C_D = 0$ and $f = 0.01$, indicating considerably less loss of momentum in the system as a result of drag than did the secondary flow static pressure comparisons. Thrust comparisons (fig. 7(c)) indicate relatively high drag and friction losses. (The thrust ratio becomes less than 1 at higher engine speeds; this is predicted for large drag on the struts.)

The calculations show that wall friction and losses at the struts could account for as much as an 8 percent increase in secondary static pressure and for decreases of 4 and 27 percent in mixed total pressure and thrust, respectively. Additional losses may be caused by separation of the flow or by development of an excessive boundary layer in the unfavorable pressure gradient in the nozzle. Losses are probable also around the engine mount obstructions near the ejector bell-mouth inlet on the bottom side.

Noise Comparisons

In figure 8 the noise power radiated forward (0^{o} to 90^{o}) and to the rear (90^{o} to 180^{o}) of the engine and the total noise power are shown as a function of engine speed. The combined effect of an annular nozzle and an ejector caused a considerable increase (5 to 10 dB) in forward noise and a decrease (1.5 to 8 dB) in rearward noise at moderate to high engine speeds. Total noise with the ejector increased over that for the standard nozzle at lower speeds but decreased as much as 6 decibels at higher speeds. With the ejector, at the high speeds the noise radiated forward was slightly less (1 to 2 dB) than the noise radiated rearward. At the low speeds the forward noise was about 6 decibels more than the rearward. A possible explanation is that much more noise was generated internally than externally. At low speeds, the internal noise radiated primarily out the bell-mouth inlet, which was near this mixing region; at higher engine speeds, the higher gas velocity in the ejector tended to convect this internal noise to the exhaust of the ejector, so that it radiated more in the exhaust direction.

The calculated PWL shown in figure 9 tend to corroborate this view. Predicted internal mixing noise power was 20 to 25 decibels above the external noise. For the standard nozzle the calculated noise power increased faster with engine speed (and gas velocity) than the measured noise power. This may indicate a lower velocity dependence than the eighth power used in the calculations. In these calculations the flow parameters were found by the application of the conservation equations for mass, momentum, and energy between the unmixed and fully mixed flows. The momentum equation included a friction factor of 0.01 for the ejector and centerbody walls and a drag coefficient of 1.0 for the struts in the flow passages. The calculations predict that, with less drag or friction, the velocity of the secondary flow would increase (static pressure decrease as in fig. 7(a)) so that internal noise would diminish. More complete mixing would have also resulted in higher secondary flow velocity. The relative velocity between primary and secondary flows would then be less, resulting in less internal noise. Details of the noise calculation are included in the description of the ejector calculations in the appendix.

The angular distribution of the overall sound pressure noise levels (OASPL), (fig. 10) shows more clearly that, at high engine speeds, external noise generated by the mixed flow out of the ejector was considerably less than the jet noise from the primary jet alone. In the region of 130^{o} to 160^{o} the OASPL was reduced by 8 to 11 decibels for 90, 95, and 100 percent of maximum engine speed. On the other hand, as pointed out before, a large increase in noise level at the forward angles occurred with the ejector in use.

Figure 11 compares the spectral distribution of the noise power (PWL per 1/3-octave band) from an annular nozzle with ejector to that from a standard nozzle, for both forward and rearward directions. At each engine speed the ejector caused a sizable

reduction (≤13 dB) in rearward noise power at about 200 hertz and a large increase (~7 dB) in noise power from 500 to 600 hertz and higher. Very little attenuation occurred at the lowest frequencies. Again, these data are compatible with a view that the large amount of the higher frequency (>600 Hz) noise is generated by the internal mixing process. Instead of the 160-hertz peak of the standard nozzle, the large-diameter ejector produced low-frequency noise (~100 Hz), and the annular nozzle produced high-frequency noise (>600 Hz). These trends are predicted by the Strouhal analogy, where frequency is inversely proportional to size.

The noise power radiated in the forward direction also showed a higher frequency band peaking at about the same frequency (1000 Hz) as the higher frequency band in the exhaust. The noise power in this band was higher in the forward direction than in the rearward at 50 to 80 percent speeds. At 90 to 100 percent speeds, the higher frequency noise radiated in the rearward direction exceeded that radiated forward. However, there does not seem to be a ready explanation for the fact that the low-frequency noise radiated forward was also increased by using the ejector.

In general, the noise spectrum produced by the standard nozzle has a single peak. The annular nozzle combined with the ejector produced high- and low-frequency peaks respectively, which when combined showed a double-peaked spectrum.

SUMMARY OF RESULTS

Modification of the exhaust of a J65 turbojet engine to an annular exhaust nozzle discharging into a 5:1 area ratio ejector around a centerbody resulted in as much as 8 decibels reduction in overall noise power level (PWL) radiated to the rear of the engine. The exhaust noise power spectrum shows a reduction of as much as 13 decibels in the low-frequency range, but an increase of about 7 decibels in the higher frequency (~1000 Hz) range. The higher frequency component seemed to result from the mixing of the primary and secondary flows inside the ejector.

Better mixing, together with less drag and friction, would have resulted in more secondary flow and less internal noise.

CONCLUDING REMARKS

It appears from this study that the internal flow processes in an ejector generate enough noise to make the hard-wall ejector, even a long one, only a marginal improvement on the jet noise problem. Because of the increased noise at higher frequencies, the hard-wall ejector may cause a worse problem in terms of perceived noise level. An

obvious next step is to treat acoustically as much of the interior surface of the ejector as possible in order to attenuate this internal noise. Maximum overall noise power reductions of 10 to 15 decibels would have been achieved with this ejector if the internal noise had been totally absorbed. Areas around the secondary flow inlet should have been acoustically treated to minimize internal noise radiating from these openings.

Adequate length must be allowed for complete mixing of both primary and secondary flows within the ejector shroud. As has been reported in other studies, 20 to 30 equivalent diameters of length are required for this mixing. Hence, as much contact area as possible should be provided between the flows to promote rapid mixing. This can be done by using irregular or subdivided primary exhaust nozzles, such as lobed and multiple-tube nozzles.

It is important to minimize the number of supports and protrusions into the flow in the ejector. Where such are necessary, they should be carefully faired to give minimum drag coefficients, even though they occupy only a small fraction of the cross-sectional area for flow. Calculations indicate that internal drag losses were much larger than skin friction losses for the conditions of this study.

Lewis Research Center,
National Aeronautics and Space Administration,
Cleveland, Ohio, May 15, 1973,
765-69.

APPENDIX - CALCULATION OF EJECTOR FLOW AND NOISE

One-dimensional calculations of the flows in the ejector, similar to those in references 14 and 15, are made in this appendix. In addition, the predicted noise levels generated internally and at the exit are calculated based on a modified Lighthill parameter.

Symbols

A	nozzle exit area
C_D	drag coefficient
C_0	speed of sound at ambient conditions
D	nozzle exit diameter
D_1	inner diameter of annulus
D_2	outer diameter of annulus
F_D	drag force
F_F	friction force
f	friction factor
g	force conversion constant
k	sound power coefficient
N	noise power
P	pressure
R	gas constant
S	cross-sectional area
S_{CB}	exterior surface area of centerbody
S_{EJ}	interior surface area of ejector
S_{ST}	flow obstruction area of strut
T	gas temperature
t	shear layer thickness
U	gas velocity, axial
V	volume
V_e	volume of eddy

w weight flow

x nondimensional axial distance in jet core lengths

γ specific-heat ratio

ρ density

ω fluctuation frequency

Subscripts:

M mixed flow

P primary flow

R relative

S secondary flow

0 ambient conditions

I initial mixing region

II transition mixing region

Ejector Flow

The following equations for mass, momentum, and energy conservation are used:

$$w_P + w_S = \rho_P S_P U_P + \rho_S S_S U_S = w_M = \rho_M S_M U_M$$

$$w_P U_P + P_P S_P + w_S U_S + P_P S_S - F_F - F_D = w_M U_M + P_M S_M$$

$$w_P\left(\frac{R_P \gamma_P T_P}{\gamma_P - 1} + \frac{1}{2} U_P^2\right) + w_S\left(\frac{R_S \gamma_S T_S}{\gamma_S - 1} + \frac{1}{2} U_S^2\right) = w_M\left(\frac{R_M \gamma_M T_M}{\gamma_M - 1} + \frac{1}{2} U_M^2\right)$$

where the friction F_F and strut drag F_D are calculated from

$$F_F = \frac{f}{4} \frac{\rho_M U_M^2}{2g} (S_{EJ} + S_{CB})$$

$$F_D = \frac{C_D}{2g} \sum_i \rho_i U_i^2 S_{ST,i}$$

The summation is made with ρ_i and U_i values appropriate to each strut of blockage area $S_{ST,i}$. The primary, secondary, and mixed flow areas are illustrated in sketch a.

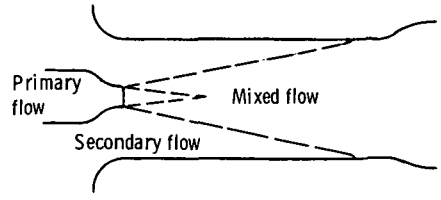

(a)

Isentropic flow is assumed before and after the mixing process. The quantity of induced secondary airflow corresponding to a given primary (engine exhaust) flow is calculated by trial and error to give a mixed flow at ambient pressure at the end of the diffuser.

Predicted Noise Levels

Jet noise for the standard nozzle and for the mixed flow out of the ejector are calculated by assuming a Lighthill noise parameter

$$N = 3\times10^{-5}\,\frac{\rho_0 U_R^8 A}{C_0^5}$$

where U_R and A refer to appropriate jet velocities and areas for the standard nozzle or ejector exit.

Internal noise is calculated by using the same modified Lighthill parameter. The velocity difference between the expanded gas from the primary and induced secondary flows is U_R. The area factor must be modified for the fact that the primary jet is annular around a centerbody instead of being a core jet.

Area Correction Factor for Annular Jet

The jet noise parameter of Lighthill (ref. 16) results from applying the expression

for noise per unit volume over the mixing region of a core jet, with appropriate frequency, eddy scale, and stress substitutions. The original result included a d^2 factor, but this is now more frequently written as an area. However, for a nozzle of the same area but different shape, a correction factor is needed.

To demonstrate this we briefly review the case of the core jet and then apply similar reasoning to the case of an annular jet with no momentum transfer at the inner surface (such as along a centerbody). The mixing region is divided into initial and transition regions which are treated separately.

The noise power per unit volume in a region of shear (ref. 16) is

$$\frac{dN}{dV} \propto \frac{V_e \omega^4 \overline{T_{ij}^2}}{\rho_0 C_0^5}$$

with $V_e \propto t^3$, $\omega \propto U/t$, and $T_{ij} \propto \rho_0 U^2$. Introducing the usual noise power coefficient k yields

$$\frac{dN}{dV} = \frac{k}{16} \frac{\rho_0 U^8}{t C_0^5}$$

Note that $1/t\ dV$ has the units of area.

Lighthill parameter for core jet. - The initial and transition mixing regions of the core jet are illustrated in sketch b.

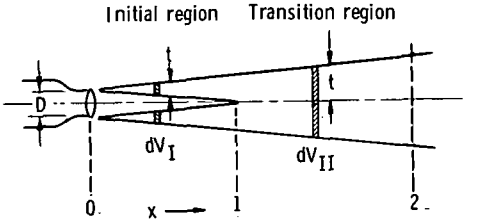

(b)

In the initial region (I) of the jet, $x = 0$ to $x = 1$, which extends to the end of the potential core,

$$dV_I = 4\pi D^3 x\, dx$$

and

$$t = xD$$

so that

$$N_I = \frac{k}{16}\frac{\rho_0 U^8}{C_0^5}\int_0^1 \frac{4\pi D^3 x}{xD}\,dx = k\,\frac{\rho_0 U^8 A}{C_0^5}$$

An approximation can be made for the transition region (II), $x = 1$ to $x = 2$, of the core jet by assuming a linear decrease in core velocity, as

$$\frac{U'}{U} = \frac{1}{5}(6 - x)$$

such that U' goes from U to $0.8\,U$ between $x = 1$ and $x = 2$. The volume element and mixing layer thickness become

$$dV_{II} = \pi D^3 (x + 1)^2\, dx$$

and

$$t = \frac{D}{2}(x + 1)$$

Then,

$$N_{II} = \frac{k}{16}\frac{\rho_0}{C_0^5}\left(\frac{2}{D}\right)\int_1^2 \left(\frac{6 - x}{5}\right)^8 (x + 1)dx = 0.5677\ k\,\frac{\rho_0 U^8 A}{C_0^5}$$

For comparison, if U' had been assumed constant and equal to U in this region, we would have had

$$N_{II} = 1.25\, k\, \frac{\rho_0 U^8 A}{C_0^5}$$

The total noise power for the core jet is then

$$N = N_I + N_{II} \approx 1.57\, k\, \frac{\rho_0 U^8 A}{C_0^5}$$

where $1.57\, k = 3\times10^{-5}$, as used in the noise calculations.

Lighthill parameter corrected for annular jet. - The initial and transition mixing regions of the annular jet are shown in sketch c.

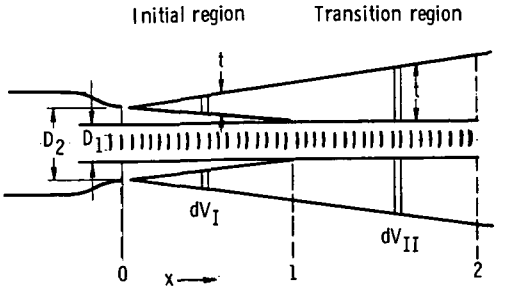

(c)

Here it is assumed that the eddy diffusivity is the same as for a core jet, so that the spreading angle is the same. No momentum is transferred to the centerbody.

In the initial region

$$dV_I = 4\pi D_2 (D_2 - D_1)^2 x\, dx$$

and

$$t = x(D_2 - D_1)$$

Then,

$$N_I = \frac{\pi}{4} k \frac{\rho_0 U^8}{C_0^5} D_2(D_2 - D_1) \int_0^1 dx = k \frac{\rho_0 U^8 A}{C_0^5} \left(\frac{D_2}{D_1 + D_2} \right)$$

where $A = \pi/4 \left(D_2^2 - D_1^2\right)$.

In the transition region

$$dV_{II} = 4\pi t(D_2 - D_1)(D_1 + t)dx$$

and

$$t = \frac{x + 1}{2} (D_2 - D_1)$$

Assuming again that $U'/U = (6 - x)/5$ in this region,

$$N_{II} = \frac{\pi}{4} k \frac{\rho_0 U^8}{C_0^5} (D_2 - D_1) \left[D_1 \int_1^2 \left(\frac{6 - x}{5} \right)^8 dx + \frac{D_2 - D_1}{2} \int_1^2 \left(\frac{6 - x}{5} \right)^8 (x + 1)dx \right]$$

$$= \frac{\pi}{4} k \frac{\rho_0 U^8}{C_0^5} \left[0.481\, D_1(D_2 - D_1) + 0.5677 \left(D_2 - D_1\right)^2 \right] = 0.57\, k \frac{\rho_0 U^8 A}{C_0^5} \left(\frac{D_2 - 0.15\, D_1}{D_2 + D_1} \right)$$

and

$$N = N_I + N_{II} = 1.57\, k \frac{\rho_0 U^8 A}{C_0^5} \left(\frac{D_2 - 0.055\, D_1}{D_2 + D_1} \right)$$

For exhaust nozzles of equal area at the same flow conditions, the annular nozzle will make less noise than the core nozzle by the factors:

$$\frac{N_{annular}}{N_{core}} = \frac{D_2}{D_1 + D_2} \qquad \text{in region I}$$

$$\frac{N_{annular}}{N_{core}} = \frac{D_2 - 0.55\,D_1}{D_1 + D_2} \approx \frac{D_2}{D_1 + D_2} \qquad \text{in combined regions I and II}$$

These correction factors are included in the calculation of internal noise in this study. For this annular nozzle, $D_2/(D_1 + D_2) = 0.567$. This corresponds to a 2.5-decibel reduction.

REFERENCES

1. North, Warren J.; and Coles, Willard D.: Effect of Exhaust Nozzle Ejectors on Turbojet Noise Generation. NACA TN 3573, 1955.

2. Coles, Willard D.; Mihaloew, John A.; and Callaghan, Edmund E.: Turbojet Engine Noise Reduction with Mixing Nozzle-Ejector Combinations. NACA TN 4317, 1958.

3. Mihaloew, James R.: Internal-Performance Evaluation of Two Fixed-Divergent-Shroud Ejectors. NASA TN D-763, 1961.

4. Kochendorfer, Fred D.; and Rousso, Morris D.: Performance Characteristics of Aircraft Cooling Ejectors Having Short Cylindrical Shrouds. NACA RM E51E01, 1951.

5. Greathouse, W. K.; and Hollister, D. P.: Air-Flow and Thrust Characteristics of Several Cylindrical Cooling-Air Ejectors with a Primary to Secondary Temperature Ratio of 1.0. NACA RM E52L24, 1953.

6. Ciepluch, Carl C.; North, Warren J.; Coles, Willard D.; and Antl, Robert J.: Acoustic, Thrust, and Drag Characteristics of Several Full-Scale Noise Suppressors for Turbojet Engines. NACA TN 4261, 1958.

7. Coles, Willard D.; Mihaloew, John A.; and Swann, William H.: Ground and In-Flight Acoustic and Performance Characteristics of Jet-Aircraft Exhaust Noise Suppressors. NASA TN D-874, 1961.

8. Richter, Gerhard; and Hoch, Rene: Concept and Characteristics of the Concorde Flight Silencer. Paper 67-391, AIAA, June 1967.

9. Samanich, N. E.; and Huntley, S. C.: Thrust and Pumping Characteristics of Cylindrical Ejectors Using Afterburning Turbojet Gas Generator. NASA TM X-52565, 1969.

10. Middleton, D.: The Noise of Ejectors. Rep. R & M-3389, Aeronautical Research Council, Gt. Britain, 1965.

11. Nagamatsu, H. T.; Sheer, R. E., Jr.; and Wells, R. J.: Supersonic Jet Exhaust Noise Reduction with Rods, Shroud, and Induced Flow. Rep. 68-C-033, General Electric Co., Jan. 1968.

12. Smith, L. Jack; Acker, Loren W.; and Feiler, Charles E.: Sound Measurements on a Full-Scale Jet-Engine Inlet-Noise-Suppressor Cowling. NASA TN D-4639, 1968.

13. Fenn, D. B.; and Jones, William L.: Over-all Performance of J65-B3 Turbojet Engine for Reynolds Number Indices from 0.8 to 0.2. NACA RM SE55C08, 1955.

14. Krenkel, A. R.; and Lipowski, H. H.: Design Analysis of Central and Annular-Jet Ejectors. Rep. P1BAL-976, Polytechnic Inst. Brooklyn (ARL-66-0210, AD-648862), Mar. 1966.

15. Huang, K. P.; and Kisielowski, E.: An Investigation of the Thrust Augmentation Characteristics of Jet Ejectors. Rep. DCR-219 Dynasciences Corp. (USAAVLABS-TR-67-8, AD-651946), Apr. 1967.

16. Lighthill, M. J.: Jet Noise. AIAA J., vol. 1, no. 7, July 1963, pp. 1507-1517.

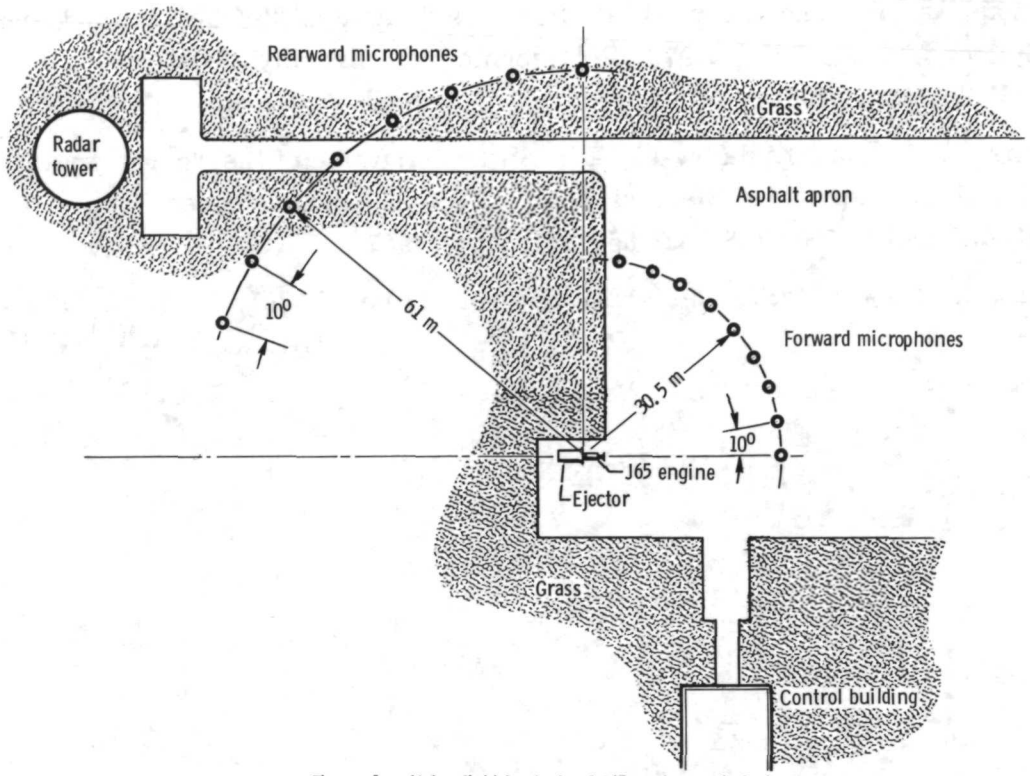

Figure 1. - Noise field for tests of J65 engine and ejector.

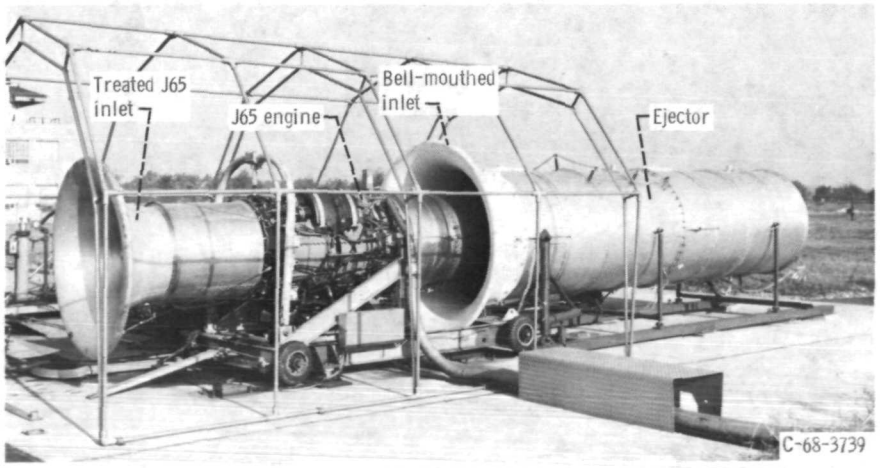

Figure 2. - Ejector and J65 engine with modified inlet.

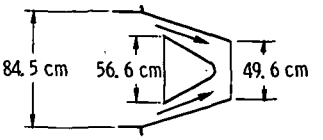

(a) J65 standard nozzle.

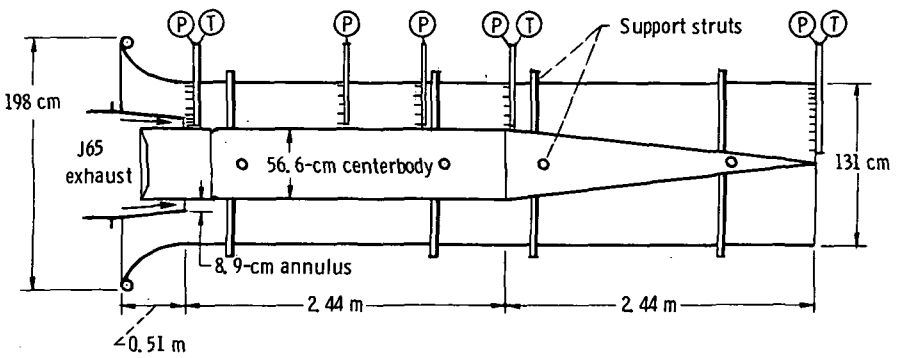

(b) Ejector for J65 engine exhaust. Ratio of mixed flow area to primary flow area, 6; ratio of exit nozzle area to mixed flow area, 1.23. Total pressure rakes and wall static pressure taps at 0, 1.22, 1.83, 2.44, and 4.88 meters from exhaust nozzle; total temperature rakes at 0, 2.44, and 4.88 meters; wall temperatures measured every 0.61 meter along length; thrust measured independent of engine.

Figure 3. - Nozzles and ejector for J65 turbojet engine.

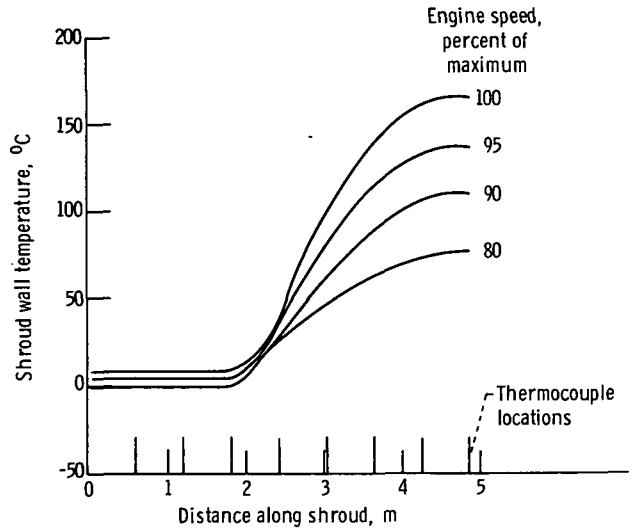

Figure 5. - Ejector shroud wall temperatures.

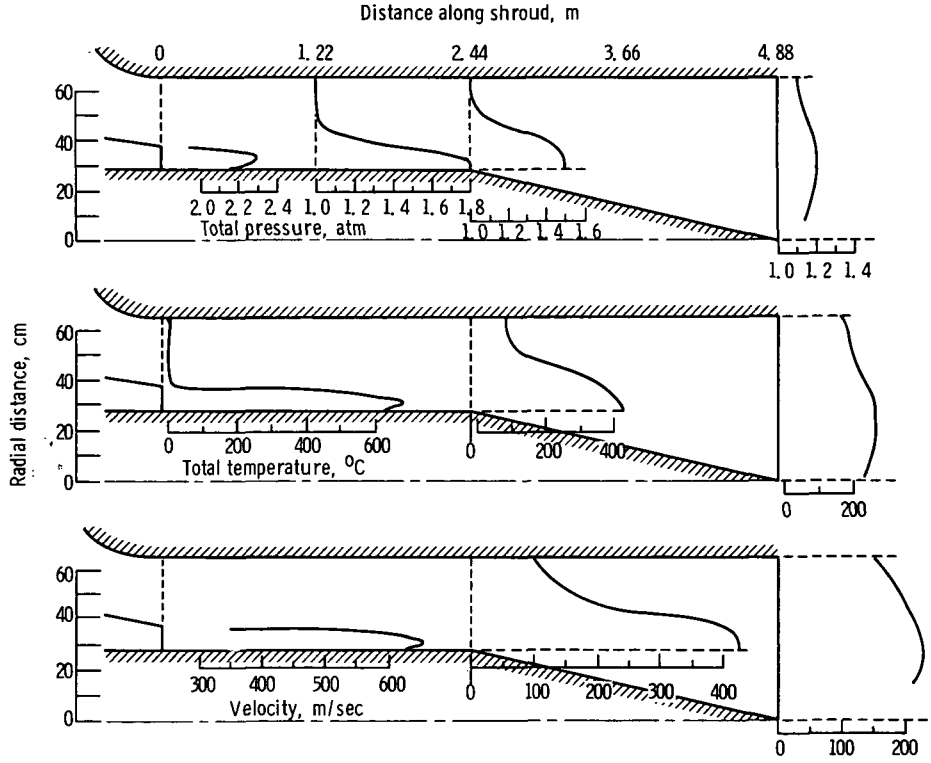

Figure 4. - Flow profiles for J65 ejector with engine at 100 percent of full speed.

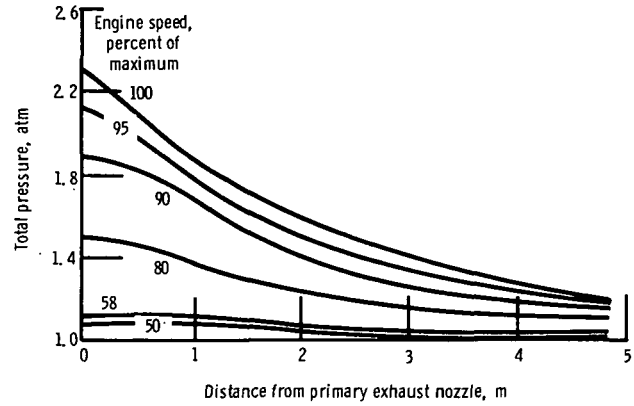

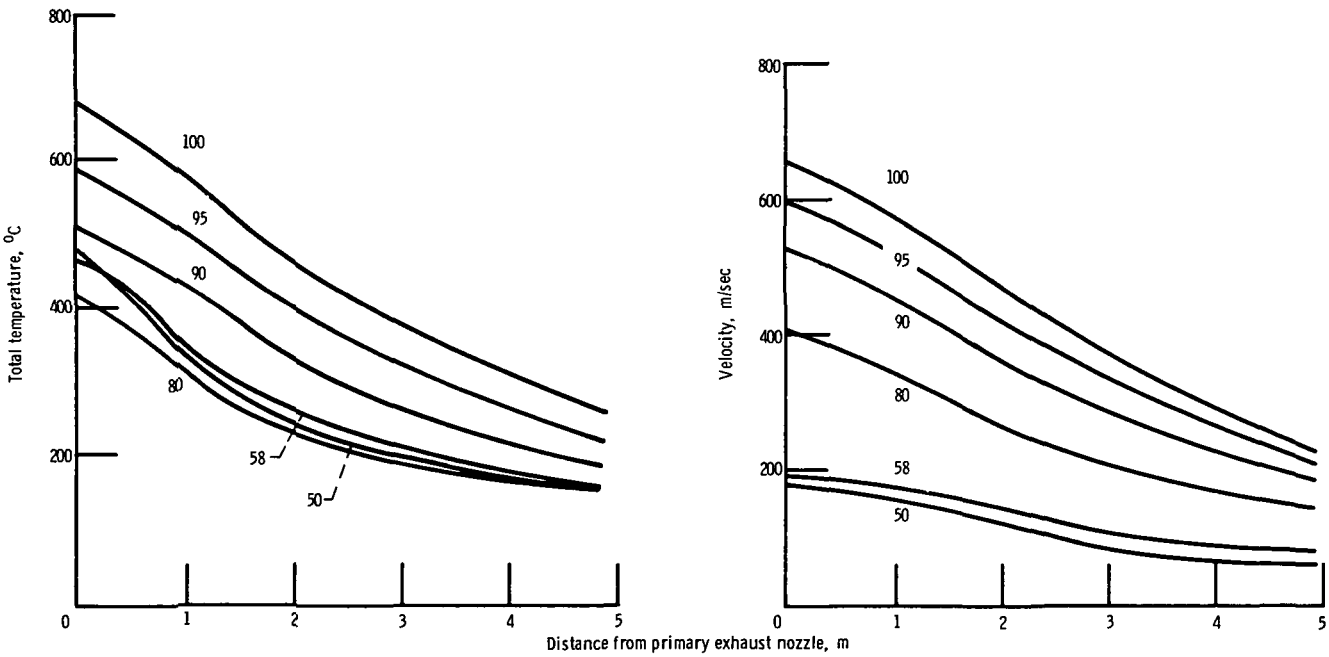

Figure 6. - Maximum values of total pressure, total temperature, and gas velocity along ejector shroud length.

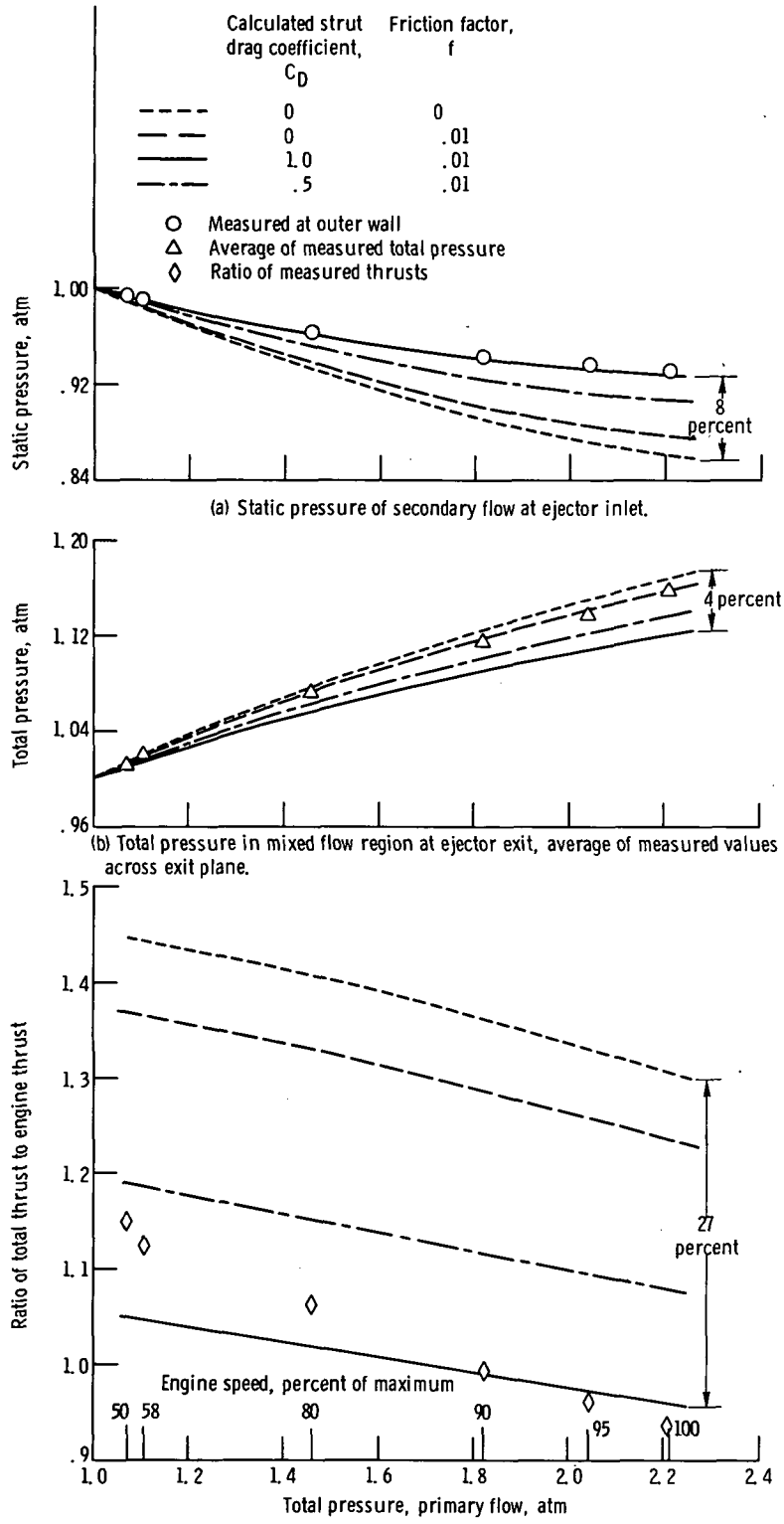

(a) Static pressure of secondary flow at ejector inlet.

(b) Total pressure in mixed flow region at ejector exit, average of measured values across exit plane.

(c) Ratio of total thrust of engine plus ejector to thrust of engine with standard nozzle.

Figure 7. - Secondary and mixed flows, calculated and measured, for J65 engine and ejector, with drag on walls and support struts.

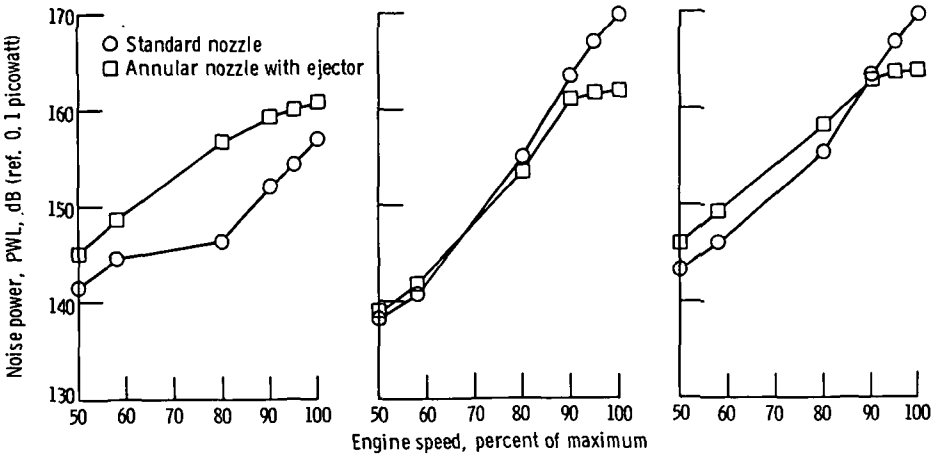

Figure 8. - Effect of ejector on noise power level (PWL) of J65 turbojet engine.

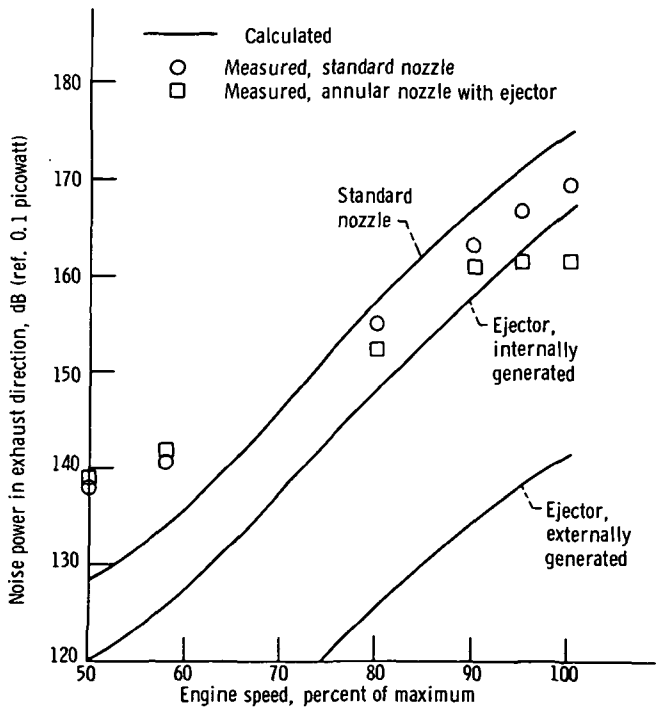

Figure 9. - Comparison of calculated and measured noise levels in exhaust direction for J65 engine and ejector. Strut drag coefficient, 1.0; wall friction factor, 0.01.

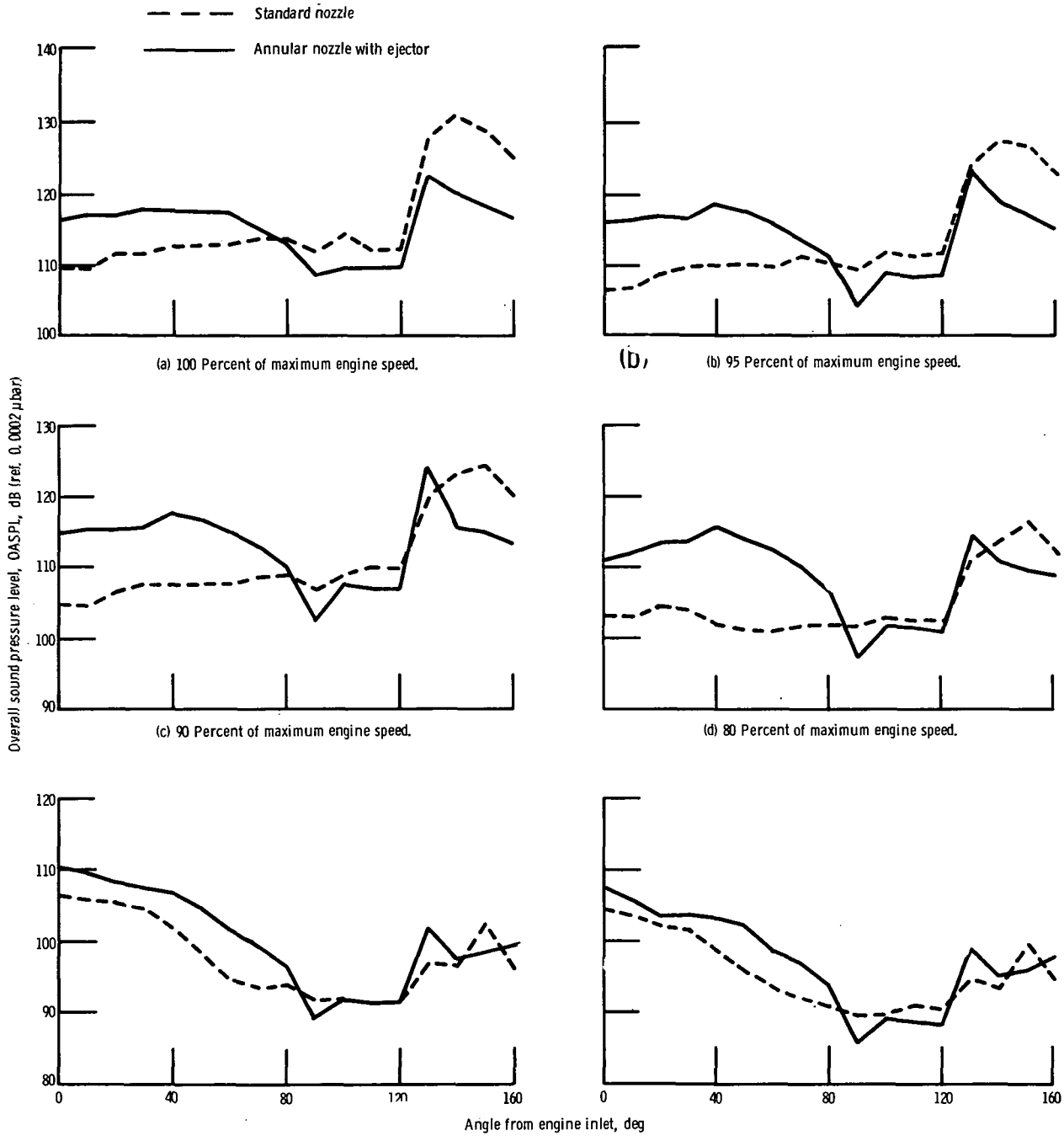

Figure 10. - Effect of engine speed on angular distribution of noise.

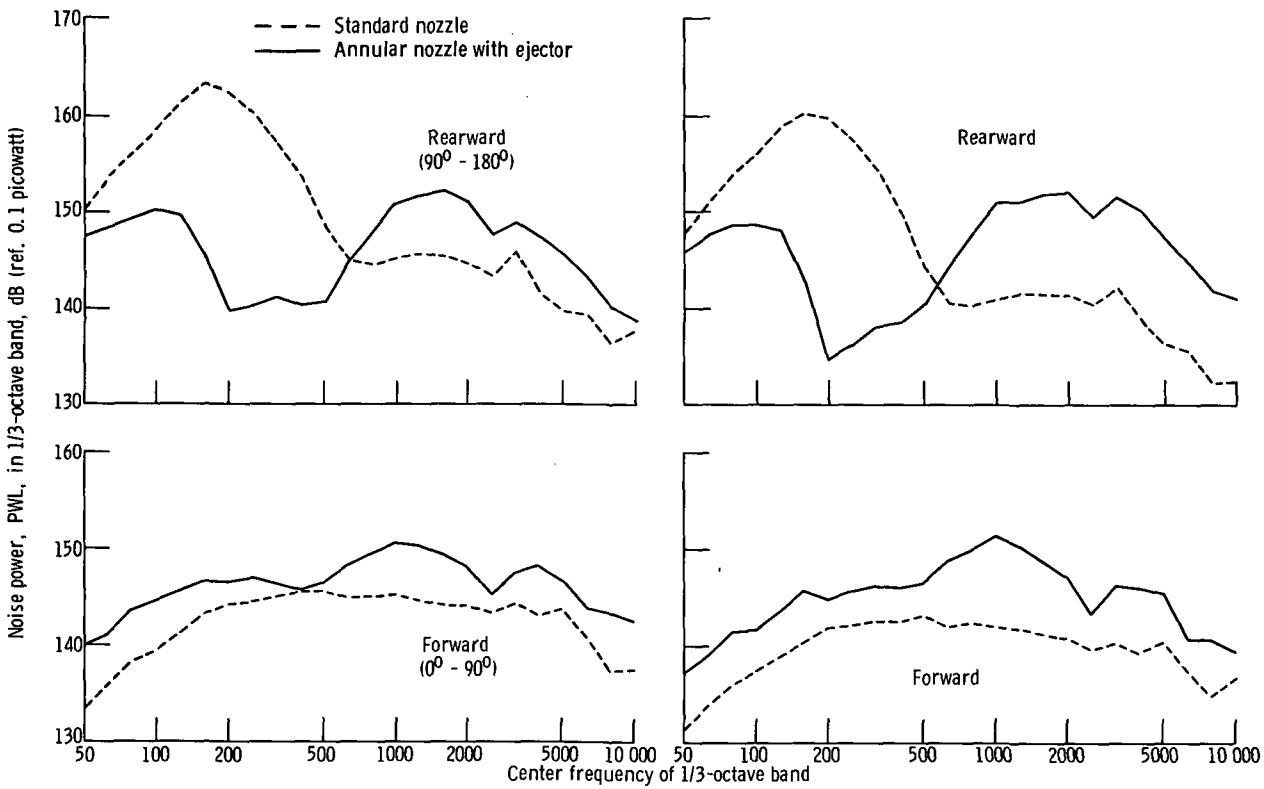

(a) 100 Percent of maximum engine speed.

(b) 95 Percent of maximum engine speed.

Figure 11. - One-third-octave spectra of noise power of J65 engine, with and without an ejector.

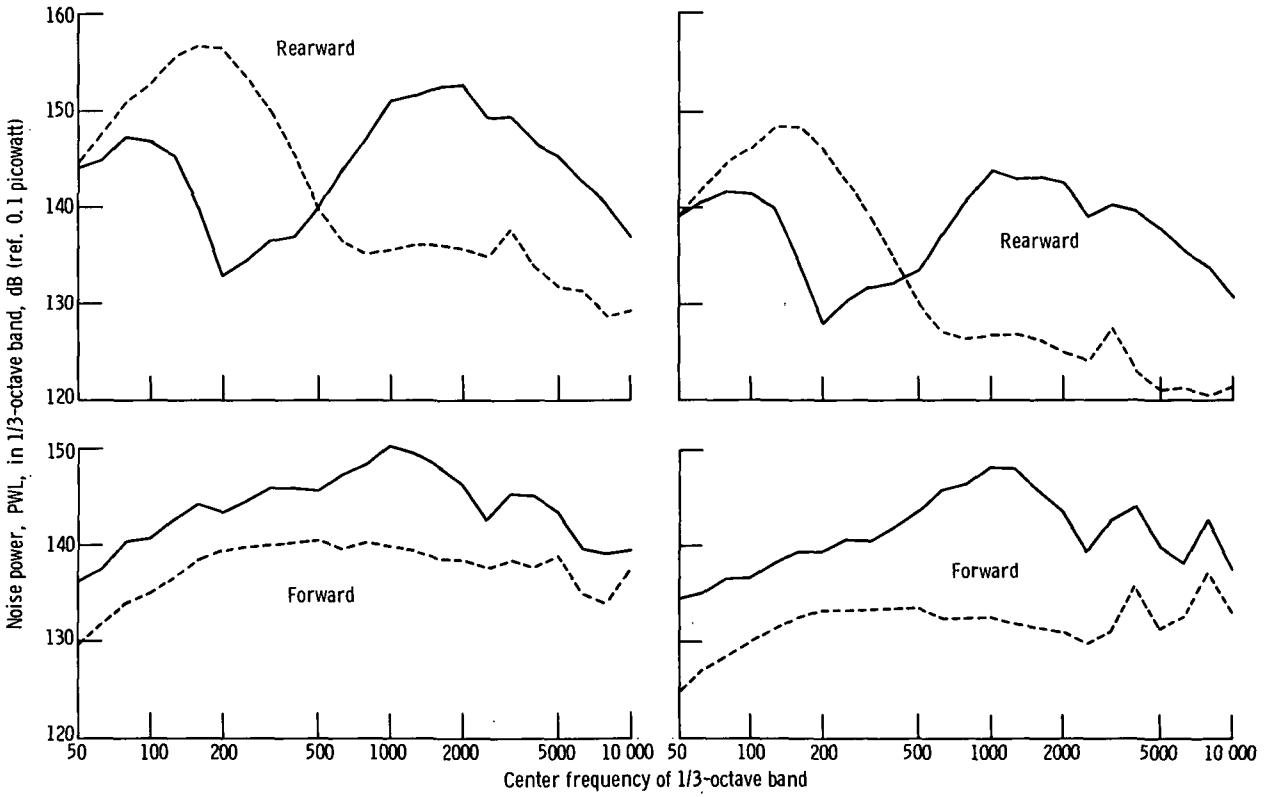

(c) 90 Percent of maximum engine speed.

(d) 80 Percent of maximum engine speed.

Figure 11. - Continued.

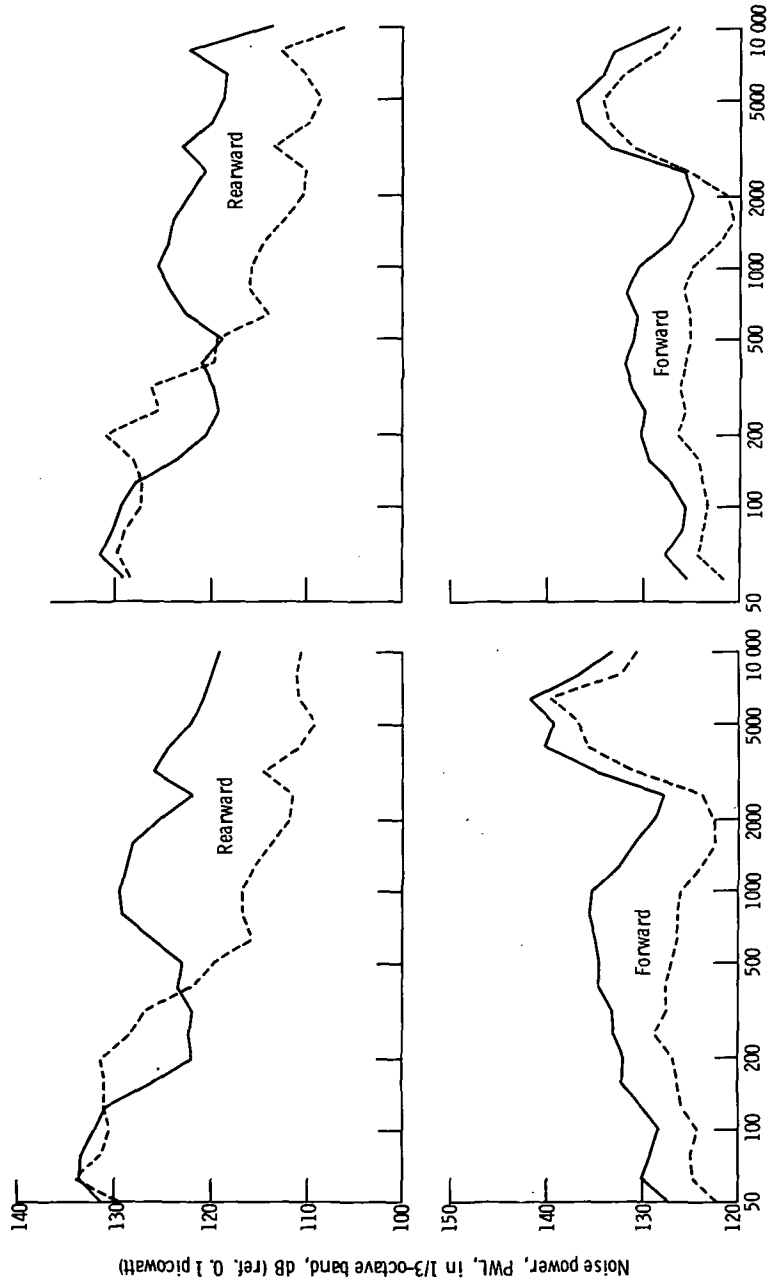

(e) 58 Percent of maximum engine speed.

(f) 50 Percent of maximum engine speed.

Figure 11. - Concluded.

NATIONAL AERONAUTICS AND SPACE ADMINISTRATION
WASHINGTON, D.C. 20546

OFFICIAL BUSINESS
PENALTY FOR PRIVATE USE $300

SPECIAL FOURTH-CLASS RATE
BOOK

POSTAGE AND FEES PAID
NATIONAL AERONAUTICS AND
SPACE ADMINISTRATION
451

U.S.MAIL

POSTMASTER: If Undeliverable (Section 158 Postal Manual) Do Not Return

"The aeronautical and space activities of the United States shall be conducted so as to contribute . . . to the expansion of human knowledge of phenomena in the atmosphere and space. The Administration shall provide for the widest practicable and appropriate dissemination of information concerning its activities and the results thereof."

—NATIONAL AERONAUTICS AND SPACE ACT OF 1958

NASA SCIENTIFIC AND TECHNICAL PUBLICATIONS

TECHNICAL REPORTS: Scientific and technical information considered important, complete, and a lasting contribution to existing knowledge.

TECHNICAL NOTES: Information less broad in scope but nevertheless of importance as a contribution to existing knowledge.

TECHNICAL MEMORANDUMS: Information receiving limited distribution because of preliminary data, security classification, or other reasons. Also includes conference proceedings with either limited or unlimited distribution.

CONTRACTOR REPORTS: Scientific and technical information generated under a NASA contract or grant and considered an important contribution to existing knowledge.

TECHNICAL TRANSLATIONS: Information published in a foreign language considered to merit NASA distribution in English.

SPECIAL PUBLICATIONS: Information derived from or of value to NASA activities. Publications include final reports of major projects, monographs, data compilations, handbooks, sourcebooks, and special bibliographies.

TECHNOLOGY UTILIZATION PUBLICATIONS: Information on technology used by NASA that may be of particular interest in commercial and other non-aerospace applications. Publications include Tech Briefs, Technology Utilization Reports and Technology Surveys.

Details on the availability of these publications may be obtained from:

SCIENTIFIC AND TECHNICAL INFORMATION OFFICE

NATIONAL AERONAUTICS AND SPACE ADMINISTRATION

Washington, D.C. 20546